Differential in vitro interactions of the Janus kinase inhibitor ruxolitinib with human SLC drug transporters

Arnaud Bruyère, Marc Le Vée, Elodie Jouan, Stephanie Molez, Anne T Nies, Olivier Fardel

Differential *in vitro* interactions of the Janus kinase inhibitor ruxolitinib with human SLC drug transporters

Arnaud Bruyère [1], Marc Le Vée [1], Elodie Jouan [1], Stephanie Molez [1], Anne T Nies [2 3], Olivier Fardel [4]

1 - Univ Rennes, Inserm, EHESP, Irset (Institut de recherche en santé, environnement et travail) - UMR_S 1085, Rennes, France.

2 - Dr. Margarete Fischer-Bosch Institute of Clinical Pharmacology, Stuttgart and University of Tübingen, Stuttgart, Germany.

3 - iFIT Cluster of Excellence (EXC2180) "Image Guided and Functionally Instructed Tumor Therapies", University of Tübingen, Tübingen, Germany.

4 - Univ Rennes, CHU Rennes, Inserm, EHESP, Irset (Institut de recherche en santé, environnement et travail) - UMR_S 1085, Rennes, France.

Abstract

1. Interactions of the Janus kinase (JAK) inhibitor ruxolitinib with solute carriers (SLCs) remain incompletely characterized. The present study was therefore designed to investigate this issue.

2. The interactions of ruxolitinib with SLCs were analyzed using transporter-overexpressing HEK293 cells. Substrate accumulation was detected by spectrofluorimetry, LC-MS/MS spectrometry or scintillation counting.

3. Ruxolitinib was found to potently inhibit the activities of OAT3, OCT2, MATE1 and MATE2-K (IC_{50} < 10 µM). It blocked OAT1, OAT4, OATP1B1, OATP1B3, OATP2B1 and OCT3, but in a weaker manner (IC_{50} > 10 µM), whereas OCT1 was not impacted. No time-dependent inhibition was highlighted. When applying the US FDA criteria for transporters-related drug-drug interaction risk, OCT2 and MATE2-K, unlike MATE1 andOAT3, were predicted to be *in vivo* inhibited by ruxolitinib. Cellular uptake studies additionally indicated that ruxolitinib is a substrate for MATE1 and MATE2-K, but not for OAT3 and OCT2.

4. Ruxolitinib *in vitro* blocked activities of most of SLC transporters. Only OCT2 and MATE-2K may be however clinically inhibited by the JAK inhibitor, with the caution for OCT2 that *in vitro* inhibition data were generated with a FDA-non recommended fluorescent substrate. Ruxolitinib MATEs-mediated transport may additionally deserve attention for its possible pharmacological consequences in MATE-positive cells.

Key-words: ruxolitinib, SLC transporter, inhibition, substrate, OCT2, MATE

Introduction

The use of Janus Kinase (JAK) inhibitor drugs, termed JAKinibs, constitutes a recent therapeutic strategy targeting immune and inflammatory diseases, as well as myeloproliferative neoplasms (Schwartz *et al.* 2017, Vainchenker *et al.* 2018). One of these JAKinibs, *i.e.*, ruxolitinib exhibits potent anti-JAK1 and anti-JAK2 activity (Quintás-Cardama *et al.* 2011) and usually considered as a pan-JAK inhibitor (Febvre-James *et al.* 2018). It was initially approved by the US Food and Drug Administration (FDA) in 2011 for myelofibrosis and polycythemia vera treatment and more recently in 2019 for that of steroid-refractory acute graft-versus-host disease (Przepiorka *et al.* 2019). Ruxolitinib is additionally undergoing testing for its efficacy in treating the cytokine storm occurring during COVID-19 infection (Malavolta *et al.* 2020). Ruxolitinib acts as an ATP-competitive JAKinib and its 7H-pyrrolo[2,3-d]pyrimidine hinge binding motif is thought to be required for its activity (Gehringer *et al.* 2014).

Membrane drug transporters are considered to play a key role in pharmacokinetics of xenobiotics and endogenous compounds. They notably contribute to the role of barrier of some tissues like gut or brain capillary endothelium, especially thanks to ATP Binding Cassette (ABC) transporters, acting as efflux pumps. Barrier and detoxifying organs also contain Solute Carrier (SLC) transporters, allowing mainly influx transport of xenobiotics, with only few of them, like multidrug and toxin extrusion proteins (MATEs/*SLC47A*), acting *in vivo* as efflux transporters (Kusakizako *et al.* 2019). Both ABC efflux and SLC influx transporters can be responsible of drug-drug interactions (DDIs), through inhibition (by perpetrators) of the transport of drugs (considered as victims) (Gessner *et al.* 2019). Their studies are now required during the development of a new chemical entity (NCE) by most of drug agencies (The International Transporter Consortium 2010, Kusakizako *et al.* 2019). The list of these transporters which have to be regulatory considered is growing, with the addition of emergent transporters like MATEs (U.S. Department of Health and Human Services, FDA 2017).

While the ruxolitinib metabolism pathway is rather well-characterized (ruxolitinib is mainly metabolized by cytochrome P450 3A4 (CYP3A4) and to a lower extent by CYP2C9 (Ogama *et al.* 2013, Shi *et al.* 2012, Agarwal *et al.* 2013)), its interaction with transporters remains to date less documented and some conflicting results about this issue have been reported. Thus, the ABC transporters P-glycoprotein (P-gp/*ABCB1*) and breast cancer resistance protein (BCRP/*ABCG2*) have initially been reported to not interact with ruxolitinib (Agarwal *et al.* 2013), but other data do not agree with this conclusion (Shi *et al.* 2015, Ebert *et al.* 2016, Gay *et al.* 2017). In the same way, SLC transporters, such as organic anion-transporting polypeptides (OATPs/*SLCOs*) and organic cation/organic anion transporters (OCTs and OATs /*SLC22A* family), were initially thought to not *in vivo* interact with ruxolitinib (Agarwal *et al.* 2013), but moderate *in vitro* inhibitions of OATP1B1 (*SLCO1B1*) or of OCT2 (*SLC22A2*) have been recently described when using ruxolitinib at 10 µM (Hu *et al.* 2014, Sprowl *et al.* 2016), a concentration closed to those reached *in vivo* (Shi *et al.* 2011). Besides, the putative inhibitions by the JAKinib of MATEs and other emergent transporters, such as OCT3, sharing many substrates with OCT1 and OCT2 (Koepsell 2020), and OAT4, which may be implicated in renal reabsorption of drugs (Burckhardt 2012), have not yet been investigated, according to the best of our knowledge. The possible transport of ruxolitinib by SLCs remains also poorly characterized (Alim *et al.* 2020). Therefore, even if some data about interactions of ruxolitinib with drug transporters are freely available online (Center for Drug Evaluation and Research 2011), additional studies about this topic are likely needed to confirm and extend previous results, notably with respect to emergent SLC transporters, including MATEs. Such studies may use fluorescent reference substrates for some transporter inhibition assays, which does not requires the use of high-cost and specific analytical methods like scintillation counting or liquid chromatography coupled to tandem mass spectrometry (LC-MS/MS) (Fardel *et al.* 2015). The present work was therefore designed to evaluate ruxolitinib interactions with main

SLC drug transporters, including emergent ones, implicated in pharmacokinetics, using partly fluorescent substrates for some of the transporter inhibition assays, and to compare results with those previously obtained. Our data highlighted potential clinical inhibition of OCT2 by ruxolitinib and also transport of the JAKinib by MATEs.

Materials and Methods

Chemicals

4′,5′-dibromofluorescein (DBF), 2′,7′-dichlorofluorescein (DCF), 6-carboxyfluorescein (6-CF), amitriptyline, corticosterone, probenecid, rifamycin SV, sulfobromophthalein (BSP) and tetraethylammonium (TEA) were from Sigma-Aldrich (Saint Quentin Fallavier, France), 4-(4-(dimethylamino)styryl)-N-methylpyridiniumiodide (4-Di-ASP) from Thermo Fisher Scientific (Waltham, MA) and 8-fluorescein-cAMP (8-FcA) from BioLog Life Science Institute (Bremen, Germany). [6,7-^{3}H(N)]- estrone-3-sulfate (E3S) (specific activity of 54 Ci/mmol) was provided by PerkinElmer (Boston, MA). Stocked solutions of chemicals were commonly prepared in dimethyl sulfoxide (DMSO); final concentrations of solvent in transport assay medium did not exceed 0.1 % (vol/vol).

Cell culture

Human embryonic kidney cell line (HEK293 cells) stably overexpressing OAT1 (HEK-OAT1 cells), OAT3 (HEK-OAT3 cells), OAT4 (HEK-OAT4 cells), OATP1B1 (HEK-OATP1B1), OATP1B3 (HEK-OATP1B3), OATP2B1 (HEKOATP2B1 cells), OCT1 (HEK-OCT1 cells), OCT2 (HEK-OCT2 cells), OCT3 (HEK-OCT3 cells), MATE1 (HEK-MATE1 cells) or MATE2-K (HEK-MATE2-K cells), as well as control HEK293-MOCK cells were cultured in DMEM medium (Thermo Fisher Scientific, Villebon sur Yvette, France) containing 4.5 g/L D-glucose and supplemented with 10% fetal calf serum (vol/vol), 1 µg/mL bovine insulin (Sigma-

Aldrich), 1% non-essential amino acid solution (Thermo Fisher Scientific), 20 UI/mL penicillin and 20 µg/mL streptomycin. G418 (800 µg/mL) was added for the culture of HEK-OCT3 cells, as a selection agent. All these SLC transporter-overexpressing HEK293 cells have previously been described and validated (Sayyed *et al.* 2019, Nies *et al.* 2011, Chedik *et al.* 2017).

For functional transport assays, cells were plated in 48-wells or 96-wells plates coated with poly-D-lysine to enhance cell adhesion, at a density of $4x10^4$ or $1x10^4$ cells/well, respectively, and were used when reaching confluence (usually 5 days after seeding).

Transporter assays

Transporter assays were performed as previously described (Chedik *et al.* 2017). Briefly, for *cis*-inhibition studies, cells were incubated for 5 min at 37°C in a transport assay buffer containing a reference substrate of the considered transporter, in the presence or absence of a reference inhibitor or ruxolitinib. The 5 min incubation time was already demonstrated to be in the linear uptake range for transporters and is commonly used for transport assays with HEK-293 cell lines (Le Vée *et al.* 2019, Jouan *et al.* 2014, Fardel *et al.* 2015, Müller *et al.* 2013). For the determination of potential time-dependent inhibition, ruxolitinib pre-incubation was performed for 30 min as recommended by the 2017 US FDA guidance entitled "In Vitro Metabolism- and Transporter- Mediated Drug-Drug Interaction Studies Guidance for Industry" (U.S. Department of Health and Human Services, FDA 2017) . The assay buffer consisted in 136 mM NaCl, 5.3 mM KCl, 1.1mM KH_2PO_4, 0.8 mM $MgSO_4$, 1.8 mM $CaCl_2$, 10 mM HEPES and 11 mM D-glucose, adjusted to pH=7.4 (8.4 for organic cation/proton exchangers MATEs). The nature and concentrations of substrates and inhibitors used for each investigated SLC transporter have previously been well documented (Le Vée *et al.* 2019) and are summarized in Table 1. Cells were next washed twice with ice-cold phosphate-buffered saline (PBS), and lysed in distilled water. Intracellular accumulation of reference substrates was finally determined by

scintillation counting using a Tri-Carb© 2910TR analyser (PerkinElmer) for [^{3}H]-E3S or by spectrofluorimetry using a SpectraMax Gemini SX spectrofluorometer (Molecular Devices, Sunnyvale, CA, USA) for 6-CF, DBF, DCF, 8-FcA and 4-Di-ASP; preliminary experiments indicated that ruxolitinib did not decrease transporter probes-related fluorescence in HEK-MOCK cells (Figure S1), thus supporting the absence of major analytical interference of the JAKinib with the fluorescent dyes used as substrates in a cellular context. LC-MS/MS, based on a high-performance liquid chromatography Aria system (Agilent, Les Ulis, France), equipped with a Poroshell 120 C18 (4.6 × 100 mm) column (Agilent, Les Ulis, France) and coupled to a tandem mass spectrometry TSQ Vantage (Thermo Fisher Scientific, Villebon sur Yvette, France), fitted with an electrospray ionization source (ESI+), was additionally used for analyzing unlabeled TEA; monitored ion transitions were at 130.2 > 86.1 m/z. Data were then normalized to total protein content, determined by the Bradford's method (Bradford 1976). Data were routinely expressed as percentages of substrate accumulation found in the absence of ruxolitinib or reference inhibitors according to the following equation (A):

$$\%\ \text{Substrate accumulation} = \frac{([\text{Substrate}_{\text{ruxolitinib or inhibitor}}]) \times 100}{([\text{Substrate}_{\text{control}}])} \qquad \text{(A)}$$

with [Substrate $_{\text{ruxolitinib or inhibitor}}$] = cellular concentration of reference substrate in the presence of a defined concentration of ruxolitinib or reference inhibitor and [Substrate $_{\text{control}}$] = cellular concentration of reference substrate in cells not exposed to ruxolitinib or reference inhibitor.

Some data were also expressed as % of residual SLC transporter activity according to the following equation (B):

$$\%\ \text{Transporter activity} = \frac{([\text{Substrate}_{\text{ruxolitinib}}] - [\text{Substrate}_{\text{ref inhibitor}}]) \times 100}{([\text{Substrate}_{\text{control}}] - [\text{Substrate}_{\text{ref inhibitor}}])} \qquad \text{(B)}$$

with [Substrate $_{\text{ruxolitinib}}$] = cellular concentration of reference substrate in the presence of a defined concentration of ruxolitinib, [Substrate $_{\text{ref inhibitor}}$] = cellular concentration of reference substrate in the presence of a defined concentration of reference inhibitor and [Substrate $_{\text{control}}$]

= cellular concentration of reference substrate in cells not exposed to ruxolitinib or reference inhibitor. *[Table 1 near here]*

Determination of half maximal inhibitory concentrations (IC_{50})

IC_{50} values were determined in most cases if ruxolitinib inhibited more than 50% of a transporter activity when incubated at 10 µM. For this, the effects of various ruxolitinib concentrations (from 0.01 to 100 µM) towards activity of the incriminated transporter were determined as described above. The time-dependent inhibition, *i.e.*, the effects of 30 min pre-incubation with ruxolitinib, was also determined towards these activities according to FDA recommendations to determine a potential IC_{50} shift (U.S. Department of Health and Human Services, FDA 2020). IC_{50} values were next determined using Prism 5.0 software (GraphPad Software, La Jolla, CA, USA) through nonlinear regression based on the following four-parameter logistic equation (C):

$$A = \text{Bottom} + \frac{\text{Top} - \text{Bottom}}{1 + 10^{(\text{LogIC50} - [\text{I}])\text{x Hill slope}}} \qquad \text{(C)}$$

where A is the percentage of transporter activity for a given concentration of ruxolitinib, [I] is the ruxolitinib concentration in the medium, Hill slope is a coefficient describing the steepness of the curve and Bottom and Top are the highest and lowest residual activity, respectively (usually fixed at 0 and 100, respectively).

Ruxolitinib accumulation assays

HEK-MOCK, HEK-OAT3, HEK-MATE1, HEK-MATE2-K and HEK-OCT2 cells were incubated with 100 µM ruxolitinib, in the absence or presence of reference transporter inhibitors (2 mM probenecid, 100 µM verapamil or 100 µM amitriptyline for OAT3, MATE or OCT2 inhibition, respectively), for 5 min at 37°C, in the transport assay medium already described above. The use of the 100 µM concentration of ruxolitinib was selected for favouring analytical

determination of intracellular levels of the JAKinib. Cells were then washed twice in ice-cold PBS, lysed in distilled water and acetonitrile-based extraction of cell lysates was performed. Ruxolitinib quantification was next performed through LC-MS/MS using the system described above; ruxolitinib monitored ion transitions were at 307.1 > 186.1 m/z. Data were finally normalized to protein content determined by the Bradford's method (Bradford 1976).

Prediction of in vivo modulation of SLC transporter activity by ruxolitinib

In vivo modulation of transporter activities by ruxolotinib was evaluated from *in vitro* data using the criteria defined by the US FDA guidance on *in vitro* drug interaction studies (U.S. Department of Health and Human Services, FDA) Briefly, OAT1, OAT3, OCT2, MATE1 or MATE2-K can be *in vivo* inhibited by ruxolitinib if:

$$I_{max,\,u} / IC_{50} \geq 0.1 \qquad (D)$$

with $I_{max,u}$ = maximum unbound plasma concentration of ruxolitinib and IC_{50} = half maximal inhibitory concentration. The equation (D) was also retained for evaluating *in vivo* inhibition of OCT3 and OAT4.

For OATP1B1 and OATP1B3, expressed at the sinusoidal membrane of hepatocytes, an *in vivo* inhibition can be considered according to the US FDA if:

$$R=1+ ((f_{u,p} \times I_{in,max})/IC_{50}) \geq 1.1 \qquad (E)$$

with $f_{u,p}$ = unbound fraction in plasma, IC_{50} = half maximal inhibitory concentration and $I_{in,max}$ = estimated maximum plasma inhibitor concentration at the inlet to the liver, calculated as:

$$I_{in,max} = I_{max} +(F_a \times F_g \times k_a \times Dose)/Q_h/R_B \qquad (F)$$

with I_{max} = maximum plasma concentration of ruxolitinib, F_a = fraction absorbed, F_g = intestinal availability, k_a = absorption rate constant, Q_h = hepatic blood flow rate and R_B = blood-to-plasma concentration ratio (If unknown, F_a= 1, F_g = 1 and k_a = 0.1/min can be used as a worst-case estimate).

The equation (E) was also used for evaluating *in vivo* inhibition of OATP2B1 and OCT1, expressed notably at the sinusoidal membrane of hepatocytes (Le Vée *et al.* 2015).

Statistical analysis

Experimental data were routinely expressed as means ± standard deviations (SD). They were statistically analyzed through analysis of variance (ANOVA) followed by the Dunnett's or the Tukey's post-hoc test. IC_{50} values determined with and without pre-incubation with ruxolitinib were compared with the F-test. The criterion of significance was $p < 0.05$.

Results

Interactions of ruxolitinib with SLC transporters of anionic drugs

Ruxolitinib was first tested towards OAT activities, using HEK-OAT cells. Such cells displayed fully functional OAT activities, as demonstrated by the marked inhibition of 6-CF accumulation in HEK-OAT1 and HEK-OAT3 cells, as well as that of E3S in HEK-OAT4 cells, by the reference OAT inhibitor probenecid (Figure 1A). Ruxolitinib was found to inhibit OAT activities in a concentration-dependent manner (Figure 1A). While the JAK inhibitor used at 100 µM significantly reduced accumulation of 6-CF in HEK-OAT1 and HEK-OAT3 cells and that of E3S in HEK-OAT4 cells, the lower concentration of 10 µM failed to reduce E3S accumulation in HEK-OAT4 cells and only modestly, but significantly, decreased that of 6-CF in HEK-OAT1 cells by 36% (Figure 1A). This indicated that IC_{50} values of ruxolitinib towards OAT1 and OAT4 activities are > 10 µM (Table 2). By contrast, ruxolitinib used at 10 µM reduced 6-CF accumulation in HEK-OAT3 cells by 67% (Figure 1A). IC_{50} values towards OAT3 activity were estimated at 3.1 ± 1.4 µM (without pre-incubation) and 2.9 + 1.1 µM (with a 30 min-pre-incubation) (Figure 1B), indicating no time-dependent inhibition ($p>0.05$). Similar accumulation of ruxolitinib in HEK-OAT3 and HEK-MOCK cells was further

demonstrated by LC-MS/MS analysis, without any significant effect of the OAT inhibitor probenecid (Figure 1C). This supports a lack of transport of ruxolitinib by OAT3. *[Figure 1 and Table 2 near here]*

The effects of ruxolitinib towards SLC transporter activities were next characterized in HEK-OATP cells. OATPs were fully active in such cells, as demonstrated by the significant inhibitions of the cellular accumulations of reference OATP substrates (DCF, 8-FcA and DBF for OATP1B1, OATP1B3 and OATP2B1, respectively) by the OATP inhibitors BSP and rifamycin SV (Figure 2A). Ruxolitinib used at 100 μM markedly inhibited accumulation of the reference OATP substrates in HEK-OATP1B1, HEK-OATP1B3 and HEK-OATP2B1 cells (Figure 2A); the concentration of 10 μM however failed to reduce substrate accumulation in HEK-OATP1B3 and HEK-OATP2B1 cells and only weakly, but significantly, decreased it in HEK-OATP1B1 cells by 32%. This indicated that IC_{50} values of ruxolitinib towards activities of OATP1B1, OATP1B3 and OATP2B1 are > 10 μM (Table 2). For OATP1B1, IC_{50} value was determined at 14.2 ± 1.1 μM without pre-incubation with ruxolitinib (Figure 2B); with a 30 min pre-incubation, IC_{50} value (12.2 ± 1.1 μM) was not statistically different *[Figure 2 near here]*

Interactions of ruxolitinib with SLC transporters of cationic drugs

The effects of ruxolitinib towards OCT activities were determined in HEK-OCT cells, displaying functional OCT activities, as demonstrated by the inhibition of 4-Di-ASP accumulation by the reference OCT inhibitors amitriptyline and corticosterone (Figure 3A). Ruxolitinib used at 10 or 100 μM failed to alter 4-Di-ASP accumulation in HEK-OCT1 cells (Figure 3A), indicating that it was ineffective towards OCT1 (IC_{50} > 100 μM) (Table 2). It significantly reduced 4-Di-ASP uptake in HEK-OCT3 cells, but only when used at 100 μM (Figure 3A), therefore supporting a ruxolitinib IC_{50} > 10 μM towards OCT3 activity (Table 2). The JAK inhibitor more markedly inhibited 4-Di-ASP accumulation in HEK-OCT2 cells, with

a near full inhibition of the cellular accumulation of the reference OCT substrate in response to 10 and 100 µM ruxolitinib (Figure 3A). Ruxolitinib IC_{50} values towards OCT2 activity were further determined to be 1.2 ± 1.3 µM (without pre-incubation) and 1.7 ± 1.2 µM (with pre-incubation) (Figure 3B), indicating the absence of time-dependent inhibition ($p>0.05$). Similar accumulation of ruxolitinib in HEK-OCT2 and HEK-MOCK cells was finally demonstrated by LC-MS/MS analysis, without any significant effect of the OCT inhibitor amitriptyline (Figure 3C). This most likely indicates that ruxolitinib is not transported by OCT2. *[Figure 3 near here]*

Ruxolitinib inhibitory properties were next tested in HEK-MATE1 and HEK-MATE2-K cells. These HEK-MATE cells exhibited functional MATE activities, as assessed by the verapamil-inhibited accumulation of the reference MATE substrate TEA (Figure 4A). Ruxolitinib used at 10 or 100 µM was found to markedly inhibit TEA accumulation in HEK-MATE1 and HEK-MATE2-K cells, by more than 60 % in response to the 10 µM concentration (Figure 4A). IC_{50} values towards MATE1 and MATE2-K activities in the absence of pre-incubation were next estimated to 2.5 ± 1.8 µM and 1.1 ± 1.2 µM, respectively (Figure 4B), without any significant impact of pre-incubation step (IC_{50} values after a 30 min-preincubation were 2.3 ± 1.6 and 1.0 ± 1.14 µM for MATE1 and MATE2-K, respectively). HEK-MATE1 and HEK-MATE2-K cells were then demonstrated to display enhanced cellular accumulation of ruxolitinib when compared to HEK-MOCK cells (by 3.2- and 3.8-fold factors for HEK-MATE1 and HEK-MATE2-K cells, respectively) (Figure 4C). Co-incubation of verapamil suppressed this increased ruxolitinib accumulation in HEK-MATE1 and HEK-MATE2-K cells, without affecting ruxolitinib levels in HEK-MOCK cells (Figure 4C). Such data support a transport of ruxolitinib by MATE1 and MATE2-K. *[Figure 4 near here]*

Prediction of in vivo inhibition of SLC transporters by ruxolitinib

Potential *in vivo* inhibition of SLC transporter activities by ruxolitinib was predicted using the criteria defined by the US FDA for transporters-related DDIs. We obtained a maximal plasma concentration (I_{max}) of 7.2 µM for ruxolitinib, whose unbound fraction is 0.03, according to US FDA data (Center for Drug Evaluation and Research 2011). This resulted in a $I_{max,u}$ value of 0.216 µM for ruxolitinib. With such an $I_{max,u}$ and the IC_{50} values determined in the present study using reference (like TEA) or fluorescent substrates, the ratio $I_{max,u}/IC_{50}$ reached the threshold of 0.1 for only OCT2 and MATE2-K, indicating that these transporters were susceptible to be *in vivo* blocked by ruxolitinib, unlike OCT3, OATs and MATE1 (Table 2). For OATPs and OCT1, we calculated an $I_{in,max}$ = 17.7 µM (with I_{max} = 7.2 µM at Dose = 200 mg; F_a = 0.99, F_g = 0.87, k_a = 2.02 h^{-1} and R_B = 1.2 according to Umehara et al. (Umehara *et al.* 2019)). This led to R values lower than 1.1 for OCT1, OATP1B1, OATP1B3 and OATP2B1, discarding any *in vivo* inhibition of OCT1 or OATPs by ruxolitinib (Table 2).

Comparison with FDA data for in vitro SLC transporter inhibition by ruxolitinib

We finally compared data from our present study to those from the FDA report on ruxolitinib (Center for Drug Evaluation and Research 2011), with respect to ruxolitinib-mediated *in vitro* inhibition of OATs, OATPs and OCTs. As shown in Table 3, 4/6 transporters, *i.e.*, OAT3, OATP1B1, OATP1B3 and OCT2, were found to be inhibited by ruxolitinib in the two studies. According to IC_{50} values, OCT2 was however almost 10-fold more sensitive to ruxolitinib in our study (based on 4-Di-ASP transport) than in that reported by the FDA (based on 1-methyl-4-phenylpyridinium transport). Divergent *in vitro* effects of ruxolitinib were reported for 2/6 transporters: (i) OAT1, which is rather moderately inhibited by ruxolitinib in our study, was not sensitive to ruxolitinib in the FDA report, knowing however that the maximal tested concentration in the FDA report was 37.5 µM (versus 100 µM in our study) and (ii) OCT1, inhibited by ruxolitinib according to the FDA (with an IC_{50} < 10 µM), was not impaired by

ruxolitinib, even at the high concentration of 100 µM, in our present work (Table 3). *[Table 3 near here]* It is however noteworthy that the OAT1 and OCT1 substrates used in our study (fluorescent substrates like 6-CF and 4-Di-ASP) were different from those used in the FDA report (aminohippuric acid and 1-methyl-4-phenylpyridinium).

Discussion

The present study demonstrates that the JAK inhibitor ruxolitinib differentially *in vitro* interacts with the main SLC drug transporters. If ruxolitinib used at the high concentration of 100 µM was able to inhibit most of SLC transporters usually implicated in drug pharmacokinetics (at absorption and/or distribution and/or elimination steps), such as OAT1, OAT3, OATP1B1, OATP1B3, OATP2B1, OCT2, MATE1 and MATE2-K, only activities of OAT3, OCT2, MATE1 and MATE2-K were suppressed with ruxolitinib $IC_{50} < 10$ µM. In addition, when applying the criteria of FDA for clinical prediction of DDI, only OCT2 and MATE2-K are susceptible to be *in vivo* blocked by ruxolitinib. This suggests that administration of drugs substrates for OCT2 and/or MATE2-K and subjected to renal secretion, such as metformin or cimetidine (Wang *et al.* 2008), may require special attention in terms of DDI for patients already treated by ruxolitinib. By contrast, for other SLC transporters, any putative DDIs due to inhibition of transporter activity by ruxolitinib may likely be discarded.

Comparison of the data found in the present study with those previously reported by the FDA reveals some similarities, notably for OAT3, OATP1B1 and OATP1B3 (Table 3). OCT2 was also found to be inhibited by ruxolitinib in the two studies, even if this transporter was 10-fold more sensitive to ruxolitinib in our present study. In the same way, 10 µM ruxolitinib inhibited OCT2-mediated transport by approximately 80% in the present work (Figure 3A), but by only 60% in the work of Sprowl et al (2016). Such a higher *in vitro* sensitivity likely explains why *in vivo* inhibition of OCT2 by ruxolitinib was predicted to occur in the present study, but

not in the FDA report. It is noteworthy that the substrate probe used in our functional OCT2 assay (4-Di-ASP) differs from that used in the study reported by FDA (1-methyl-4-phenylpyridinium) (Table 3) and in that of Sprowl et al (2016) (TEA). This is likely to account for the differential OCT2 sensitivity to the JAK inhibitor, because the profile of OCT2 inhibition is well-known to be substrate-dependent (Belzer *et al.* 2013); in particular, OCT2-mediated 1-methyl-4-phenylpyridinium transport (used in the study of the FDA report) has been demonstrated to be less sensitive to inhibition than that of 4-Di-ASP (used in the present study) (Sandoval *et al.* 2018). This substrate-related dependence of transporter inhibition, also described for other SLC transporters like OATP1B1 (Izumi *et al.* 2013) and MATE1 (Martínez-Guerrero and Wright 2013) and for ABC transporters (Pedersen *et al.* 2017), can be hypothesized to also explain the lack of OCT1 inhibition by ruxolitinib in our study, whereas, by contrast, OCT1 activity was found to be suppressed by the JAK inhibitor in the study reported by FDA; indeed, different OCT1 substrates were used in the two studies (Table 3). The use of different substrates also likely contributes to the fact that OAT1 was inhibited by ruxolitinib in the present study, but not in the FDA report. Overall, such data highlight the importance of the substrate nature in drug transporter inhibition analyses, even if the exact clinical consequences of such substrate-dependent transporter inhibition profiles remain to be established. This supports the recent recommendation of the FDA that the inhibition constant of a tested drug should be determined with a probe substrate that may also be used in later clinical studies or, alternatively, that usually generates a lower IC_{50} for known inhibitors, to avoid underestimating the interaction potential of the investigational drug (U.S. Department of Health and Human Services, FDA 2020). In this context, fluorescent dyes may be particularly interesting to consider, because their SLC-mediated transport may be highly sensitive to inhibitors, as previously reported for OCT2-related transport of 4-DiASP (Sandoval *et al.*

2018). Additionally, inter-laboratory variability may also contribute to variability in potency (IC_{50}) of transporter inhibitors, as already underlined for P-gp inhibition (Bentz *et al.* 2013).

The capacity of ruxolitinib to inhibit the transporters MATE1, MATE2-K, OATP2B1, OAT4 and OCT3, was investigated for the first time in the present study. In this context, it is noteworthy that MATE1 and MATE2-K have to be regulatory studied during the preclinical development of new drugs (Zamek-Gliszczynski *et al.* 2018), whereas OATP2B1 is considered as a transporter of emerging clinical importance, which may therefore also be evaluated, notably in a retrospective manner (Zamek-Gliszczynski *et al.* 2018). By contrast, there is presently no regulatory recommendation for the study of OCT3 and OAT4, probably because such transporters are presently not thought to play a major role in pharmacokinetics, even if they are expressed in organs playing a main role in drug disposition such as the liver, *i.e.*, OCT3 is present at the sinusoidal membrane of hepatocytes (Nies *et al.* 2009), and the kidney, *i.e.*, OAT4 is present at the apical site of proximal tubular cells (Ekaratanawong *et al.* 2004). Ruxolitinib was found to moderately *in vitro* block OAT4 and OCT3 (inhibition in response to 100 µM ruxolitinib) and more markedly MATE1 and MATE2-K (inhibition in response to 10 µM ruxolitinib), but none of these transporters was predicted to be *in vivo* inhibited by the JAK inhibitor, with a potential exception for MATE2-K, as its R-value is higher than 0.1.

Among transporters which were rather markedly inhibited by ruxolitinib *in vitro*, *i.e.*, OAT3, OCT2, MATE1 and MATE2-K, only MATE1 and MATE2-K were found to transport the JAK inhibitor, as demonstrated by ruxolitinib accumulation assays. A contribution of OAT3 and OCT2, basically expressed at the basolateral membrane of proximal tubular cells and involved in renal secretion of drugs (Morrissey *et al.* 2013), to ruxolitinib pharmacokinetics can therefore be discarded. By contrast, MATEs, expressed at the apical membrane of hepatocytes (MATE1) and renal proximal tubular cells (MATE1 and MATE2-K) (Nies *et al.* 2016), may participate to hepatic and renal elimination of the JAK inhibitor. This putative excretion of

ruxolitinib via MATEs should however remain a minor way of elimination, as most of the drug is eliminated by the metabolic pathway (Ogama *et al.* 2013, Agarwal *et al.* 2013) and its renal secretion is very low (Shilling *et al.* 2010), thus reducing the risk of DDI due to *in vivo* inhibition of MATEs-mediated transport of the JAK inhibitor. Nevertheless, it is noteworthy that MATE1 is expressed by myeloid cells (Harrach *et al.* 2016), including macrophages (Berg *et al.* 2018), which can constitute specific targets for ruxolitinib (Febvre-James *et al.* 2018). In such cells, MATE1 may therefore be hypothesized to function as an uptake transporter for ruxolitinib, as already demonstrated for the tyrosine kinase inhibitor imatinib (Harrach *et al.* 2016). By this way, MATE1 may control the intracellular effectiveness of ruxolitinib. Further studies, investigating notably ruxolitinib accumulation in blood and bone marrow cells, are however required to validate this hypothesis.

Direct interaction with transporter activity is not the only way by which ruxolitinib may cause DDIs. Indeed, the JAK inhibitor has been reported to fully suppress interleukin (IL-6)-mediated repression of drug transporters such as OATP1B1 and OCT1, as well as that of cytochrome P-450 3A4, through antagonizing the JAK-dependent signaling cascade of IL-6 (Febvre-James *et al.* 2017). Ruxolitinib may consequently restore hepatic detoxification capacity for patients suffering from inflammatory diseases, which may in turn cause DDIs, as already described for other anti-IL-6 agents, like tocilizumab (Schmitt *et al.* 2011). Such effects are likely not restricted to IL-6, because the JAK inhibitor also prevents drug detoxifying repression triggered by IL-22 in human hepatocytes (Le Vée *et al.* 2020). Besides, ruxolitinib is likely to exert a global anti-inflammatory effect (Roskoski 2016), notably through suppressing hepatic up-regulation of acute-phase proteins like C-reactive protein (CRP) (Febvre-James *et al.* 2020) and production of inflammatory cytokines in macrophages (Febvre-James *et al.* 2018). Such a general inflammation suppression may contribute to prevent the well-

established deleterious consequences of inflammatory states with respect to drug transporter expression (Aitken *et al.* 2006).

Conclusion

To conclude, ruxolitinib was shown to differentially interact with SLC drug transporters *in vitro*. The anionic drug transporter OAT3 and the cationic drug transporters OCT2, MATE1 and MATE2-K were notably found to be inhibited by relative low concentrations of ruxolitinib ($IC_{50} < 10$ μM), but only OCT2 and MATE2-K were predicted to be *in vivo* blocked by the JAK inhibitor. MATE1 and MATE2-K, unlike OAT3 and OCT2, were additionally demonstrated to transport ruxolitinib, which may have to deserve attention, notably with respect to ruxolitinib effectiveness in MATE1-postive cells.

Conflict of interest

The authors have no conflict of interest to declare.

References

Agarwal, S., Chinn, L., and Zhang, L., 2013. An Overview of Transporter Information in Package Inserts of Recently Approved New Molecular Entities. *Pharmaceutical Research*, 30 (3), 899–910.

Ahlin, G., Karlsson, J., Pedersen, J.M., Gustavsson, L., Larsson, R., Matsson, P., Norinder, U., Bergström, C.A.S., and Artursson, P., 2008. Structural Requirements for Drug Inhibition of the Liver Specific Human Organic Cation Transport Protein 1. *Journal of Medicinal Chemistry*, 51 (19), 5932–5942.

Aitken, A.E., Richardson, T.A., and Morgan, E.T., 2006. Regulation of Drug-Metabolizing Enzymes and Transporters in Inflammation. *Annual Review of Pharmacology and Toxicology*, 46 (1), 123–149.

Alim, K., Bruyère, A., Lescoat, A., Jouan, E., Lecureur, V., Le Vée, M., and Fardel, O., 2020. Interactions of janus kinase inhibitors with drug transporters and consequences for pharmacokinetics and toxicity. *Expert Opinion on Drug Metabolism & Toxicology*, In Press.

Belzer, M., Morales, M., Jagadish, B., Mash, E.A., and Wright, S.H., 2013. Substrate-Dependent Ligand Inhibition of the Human Organic Cation Transporter OCT2. *Journal of Pharmacology and Experimental Therapeutics*, 346 (2), 300–310.

Bentz, J., O'Connor, M.P., Bednarczyk, D., Coleman, J., Lee, C., Palm, J., Pak, Y.A., Perloff, E.S., Reyner, E., Balimane, P., Brännström, M., Chu, X., Funk, C., Guo, A., Hanna, I., Herédi-Szabó, K., Hillgren, K., Li, L., Hollnack-Pusch, E., Jamei, M., Lin, X., Mason, A.K., Neuhoff, S., Patel, A., Podila, L., Plise, E., Rajaraman, G., Salphati, L., Sands, E., Taub, M.E., Taur, J.-S., Weitz, D., Wortelboer, H.M., Xia, C.Q., Xiao, G., Yabut, J., Yamagata, T., Zhang, L., and Ellens, H., 2013. Variability in P-

Glycoprotein Inhibitory Potency (IC_{50}) Using Various in Vitro Experimental Systems: Implications for Universal Digoxin Drug-Drug Interaction Risk Assessment Decision Criteria. *Drug Metabolism and Disposition*, 41 (7), 1347–1366.

Berg, T., Hegelund-Myrbäck, T., Öckinger, J., Zhou, X.-H., Brännström, M., Hagemann-Jensen, M., Werkström, V., Seidegård, J., Grunewald, J., Nord, M., and Gustavsson, L., 2018. Expression of MATE1, P-gp, OCTN1 and OCTN2, in epithelial and immune cells in the lung of COPD and healthy individuals. *Respiratory Research*, 19 (1), 68.

Bradford, M.M., 1976. A Rapid and Sensitive Method for the Quantitation of Microgram Quantities of Protein Utilizing the Principle of Protein-Dye Binding. *Analytical Biochemistry*, 72, 248–254.

Burckhardt, G., 2012. Drug transport by Organic Anion Transporters (OATs). *Pharmacology & Therapeutics*, 136 (1), 106–130.

Center for Drug Evaluation and Research, 2011. Data FDA Ruxolitinib transporters.pdf [online]. Available from: https://www.accessdata.fda.gov/drugsatfda_docs/nda/2011/202192Orig1s000ClinPharmR.pdf.

Chedik, L., Bruyere, A., Vee, M.L., Stieger, B., Denizot, C., Parmentier, Y., Potin, S., and Fardel, O., 2017. Inhibition of Human Drug Transporter Activities by the Pyrethroid Pesticides Allethrin and Tetramethrin. *PLOS ONE*, 12 (1), e0169480.

Ebert, C., Perner, F., Wolleschak, D., Schnoder, T.M., Fischer, T., and Heidel, F.H., 2016. Expression and function of ABC-transporter protein ABCB1 correlates with inhibitory capacity of Ruxolitinib in vitro and in vivo. *Haematologica*, 101 (3), e81–e85.

Ekaratanawong, S., Anzai, N., Jutabha, P., Miyazaki, H., Noshiro, R., Takeda, M., Kanai, Y., Sophasan, S., and Endou, H., 2004. Human Organic Anion Transporter 4 Is a Renal Apical Organic Anion/Dicarboxylate Exchanger in the Proximal Tubules. *Journal of Pharmacological Sciences*, 94 (3), 297–304.

Fardel, O., Le Vee, M., Jouan, E., Denizot, C., and Parmentier, Y., 2015. Nature and uses of fluorescent dyes for drug transporter studies. *Expert Opinion on Drug Metabolism & Toxicology*, 11 (8), 1233–1251.

Febvre-James, M., Bruyere, A., Le Vee, M., and Fardel, O., 2017. The JAK1/2 inhibitor ruxolitinib reverses interleukin-6-mediated suppression of drug detoxifying proteins in cultured human hepatocytes. *Drug Metabolism and Disposition*, 46 (2), 131–140.

Febvre-James, M., Lecureur, V., Augagneur, Y., Mayati, A., and Fardel, O., 2018. Repression of interferon β-regulated cytokines by the JAK1/2 inhibitor ruxolitinib in inflammatory human macrophages. *International Immunopharmacology*, 54, 354–365.

Febvre-James, M., Lecureur, V., and Fardel, O., 2020. Potent repression of C-reactive protein (CRP) expression by the JAK1/2 inhibitor ruxolitinib in inflammatory human hepatocytes. *Inflammation Research*, 69 (1), 51–62.

Gay, C., Toulet, D., and Le Corre, P., 2017. Pharmacokinetic drug-drug interactions of tyrosine kinase inhibitors: A focus on cytochrome P450, transporters, and acid suppression therapy: Pharmacokinetic interactions of TKIs. *Hematological Oncology*, 35 (3), 259–280.

Gehringer, M., Forster, M., Pfaffenrot, E., Bauer, S.M., and Laufer, S.A., 2014. Novel hinge-binding motifs for Janus kinase 3 inhibitors: a comprehensive structure-activity relationship study on tofacitinib bioisosteres. *ChemMedChem*, 9 (11), 2516–2527.

Gessner, A., König, J., and Fromm, M.F., 2019. Clinical Aspects of Transporter-Mediated Drug–Drug Interactions. *Clinical Pharmacology & Therapeutics*, 105 (6), 1386–1394.

Harrach, S., Schmidt-Lauber, C., Pap, T., Pavenstädt, H., Schlatter, E., Schmidt, E., Berdel, W.E., Schulze, U., Edemir, B., Jeromin, S., Haferlach, T., Ciarimboli, G., and Bertrand, J., 2016. MATE1 regulates cellular uptake and sensitivity to imatinib in CML patients. *Blood Cancer Journal*, 6 (9), e470–e470.

Hu, S., Mathijssen, R.H.J., de Bruijn, P., Baker, S.D., and Sparreboom, A., 2014. Inhibition of OATP1B1 by tyrosine kinase inhibitors: in vitro–in vivo correlations. *British Journal of Cancer*, 110 (4), 894–898.

Izumi, S., Nozaki, Y., Komori, T., Maeda, K., Takenaka, O., Kusano, K., Yoshimura, T., Kusuhara, H., and Sugiyama, Y., 2013. Substrate-Dependent Inhibition of Organic Anion Transporting Polypeptide 1B1: Comparative Analysis with Prototypical Probe Substrates Estradiol-17 *β* -Glucuronide, Estrone-3-Sulfate, and Sulfobromophthalein. *Drug Metabolism and Disposition*, 41 (10), 1859–1866.

Jouan, E., Le Vee, M., Denizot, C., Da Violante, G., and Fardel, O., 2014. The mitochondrial fluorescent dye rhodamine 123 is a high-affinity substrate for organic cation transporters (OCTs) 1 and 2. *Fundamental & Clinical Pharmacology*, 28 (1), 65–77.

Koepsell, H., 2020. Organic Cation Transporters in Health and Disease. *Pharmacological Reviews*, 72 (1), 253–319.

Kusakizako, T., Miyauchi, H., Ishitani, R., and Nureki, O., 2019. Structural biology of the multidrug and toxic compound extrusion superfamily transporters. *Biochimica et Biophysica Acta (BBA) - Biomembranes*, 183154.

Le Vée, M., Bacle, A., Bruyere, A., and Fardel, O., 2019. Neonicotinoid pesticides poorly interact with human drug transporters. *Journal of Biochemical and Molecular Toxicology*, 33 (10), e22379.

Le Vée, M., Bruyère, A., Jouan, E., and Fardel, O., 2020. Janus kinase-dependent regulation of drug detoxifying protein expression by interleukin-22 in human hepatic cells. *International Immunopharmacology*, 83, 106439.

Le Vée, M., Jouan, E., Denizot, C., Parmentier, Y., and Fardel, O., 2015. Analysis of Sinusoidal Drug Uptake Transporter Activities in Primary Human Hepatocytes. *In*: M. Vinken and V. Rogiers, eds. *Protocols in In Vitro Hepatocyte Research*. New York, NY: Springer, 287–302.

Malavolta, M., Giacconi, R., Brunetti, D., Provinciali, M., and Maggi, F., 2020. Exploring the Relevance of Senotherapeutics for the Current SARS-CoV-2 Emergency and Similar Future Global Health Threats. *Cells*, 9 (4), 909.

Martínez-Guerrero, L.J. and Wright, S.H., 2013. Substrate-Dependent Inhibition of Human MATE1 by Cationic Ionic Liquids. *The Journal of Pharmacology and Experimental Therapeutics*, 346 (3), 495–503.

Morrissey, K.M., Stocker, S.L., Wittwer, M.B., Xu, L., and Giacomini, K.M., 2013. Renal Transporters in Drug Development. *Annual Review of Pharmacology and Toxicology*, 53 (1), 503–529.

Müller, F., König, J., Hoier, E., Mandery, K., and Fromm, M.F., 2013. Role of organic cation transporter OCT2 and multidrug and toxin extrusion proteins MATE1 and MATE2-K for transport and drug interactions of the antiviral lamivudine. *Biochemical Pharmacology*, 86 (6), 808–815.

Nies, A.T., Damme, K., Kruck, S., Schaeffeler, E., and Schwab, M., 2016. Structure and function of multidrug and toxin extrusion proteins (MATEs) and their relevance to drug therapy and personalized medicine. *Archives of Toxicology*, 90 (7), 1555–1584.

Nies, A.T., Hofmann, U., Resch, C., Schaeffeler, E., Rius, M., and Schwab, M., 2011. Proton Pump Inhibitors Inhibit Metformin Uptake by Organic Cation Transporters (OCTs). *PLoS ONE*, 6 (7), e22163.

Nies, A.T., Koepsell, H., Winter, S., Burk, O., Klein, K., Kerb, R., Zanger, U.M., Keppler, D., Schwab, M., and Schaeffeler, E., 2009. Expression of organic cation transporters OCT1 (SLC22A1) and OCT3 (SLC22A3) is affected by genetic factors and cholestasis in human liver. *Hepatology*, 50 (4), 1227–1240.

Ogama, Y., Mineyama, T., Yamamoto, A., Woo, M., Shimada, N., Amagasaki, T., and Natsume, K., 2013. A randomized dose-escalation study to assess the safety, tolerability, and pharmacokinetics of ruxolitinib (INC424) in healthy Japanese volunteers. *International Journal of Hematology*, 97 (3), 351–359.

Pedersen, J.M., Khan, E.K., Bergström, C.A.S., Palm, J., Hoogstraate, J., and Artursson, P., 2017. Substrate and method dependent inhibition of three ABC-transporters (MDR1, BCRP, and MRP2). *European Journal of Pharmaceutical Sciences*, 103, 70–76.

Przepiorka, D., Luo, L., Subramaniam, S., Qiu, J., Gudi, R., Cunningham, L.C., Nie, L., Leong, R., Ma, L., Sheth, C., Deisseroth, A., Goldberg, K.B., Blumenthal, G.M., and Pazdur, R., 2019. FDA Approval

Summary: Ruxolitinib for Treatment of Steroid-Refractory Acute Graft-Versus-Host Disease. *The Oncologist*, theoncologist.2019-0627.

Quintás-Cardama, A., Kantarjian, H., Cortes, J., and Verstovsek, S., 2011. Janus kinase inhibitors for the treatment of myeloproliferative neoplasias and beyond. *Nature Reviews Drug Discovery*, 10 (2), 127–140.

Roskoski, R., 2016. Janus kinase (JAK) inhibitors in the treatment of inflammatory and neoplastic diseases. *Pharmacological Research*, 111, 784–803.

Sandoval, P.J., Zorn, K.M., Clark, A.M., Ekins, S., and Wright, S.H., 2018. Assessment of Substrate-Dependent Ligand Interactions at the Organic Cation Transporter OCT2 Using Six Model Substrates. *Molecular Pharmacology*, 94 (3), 1057–1068.

Sayyed, K., Camillerapp, C., Le Vée, M., Bruyère, A., Nies, A.T., Abdel-Razzak, Z., and Fardel, O., 2019. Inhibition of organic cation transporter (OCT) activities by carcinogenic heterocyclic aromatic amines. *Toxicology in vitro: an international journal published in association with BIBRA*, 54, 10–22.

Schmitt, C., Kuhn, B., Zhang, X., Kivitz, A.J., and Grange, S., 2011. Disease–Drug–Drug Interaction Involving Tocilizumab and Simvastatin in Patients With Rheumatoid Arthritis. *Clinical Pharmacology & Therapeutics*, 89 (5), 735–740.

Schwartz, D.M., Kanno, Y., Villarino, A., Ward, M., Gadina, M., and O'Shea, J.J., 2017. JAK inhibition as a therapeutic strategy for immune and inflammatory diseases. *Nature Reviews Drug Discovery*, 16 (12), 843–862.

Shi, J., Fraczkiewicz, G., Williams, W., and Yeleswaram, S., 2015. Predicting Drug-Drug Interactions Involving Multiple Mechanisms Using Physiologically Based Pharmacokinetic Modeling: A Case Study With Ruxolitinib. *Clinical Pharmacology & Therapeutics*, 97 (2), 177–185.

Shi, J.G., Chen, X., Emm, T., Scherle, P.A., McGee, R.F., Lo, Y., Landman, R.R., McKeever, E.G., Punwani, N.G., Williams, W.V., and Yeleswaram, S., 2012. The Effect of CYP3A4 Inhibition or Induction on the Pharmacokinetics and Pharmacodynamics of Orally Administered Ruxolitinib (INCB018424 Phosphate) in Healthy Volunteers. *The Journal of Clinical Pharmacology*, 52 (6), 809–818.

Shi, J.G., Chen, X., McGee, R.F., Landman, R.R., Emm, T., Lo, Y., Scherle, P.A., Punwani, N.G., Williams, W.V., and Yeleswaram, S., 2011. The Pharmacokinetics, Pharmacodynamics, and Safety of Orally Dosed INCB018424 Phosphate in Healthy Volunteers. *The Journal of Clinical Pharmacology*, 51 (12), 1644–1654.

Shilling, A.D., Nedza, F.M., Emm, T., Diamond, S., McKeever, E., Punwani, N., Williams, W., Arvanitis, A., Galya, L.G., Li, M., Shepard, S., Rodgers, J., Yue, T.-Y., and Yeleswaram, S., 2010. Metabolism, Excretion, and Pharmacokinetics of [14C]INCB018424, a Selective Janus Tyrosine Kinase 1/2 Inhibitor, in Humans. *Drug Metabolism and Disposition*, 38 (11), 2023–2031.

Sprowl, J.A., Ong, S.S., Gibson, A.A., Hu, S., Du, G., Lin, W., Li, L., Bharill, S., Ness, R.A., Stecula, A., Offer, S.M., Diasio, R.B., Nies, A.T., Schwab, M., Cavaletti, G., Schlatter, E., Ciarimboli, G., Schellens, J.H.M., Isacoff, E.Y., Sali, A., Chen, T., Baker, S.D., Sparreboom, A., and Pabla, N., 2016. A phosphotyrosine switch regulates organic cation transporters. *Nature Communications*, 7 (1), 10880.

The International Transporter Consortium, 2010. Membrane transporters in drug development. *Nature Reviews Drug Discovery*, 9 (3), 215–236.

Umehara, K., Huth, F., Jin, Y., Schiller, H., Aslanis, V., Heimbach, T., and He, H., 2019. Drug-drug interaction (DDI) assessments of ruxolitinib, a dual substrate of CYP3A4 and CYP2C9, using a verified physiologically based pharmacokinetic (PBPK) model to support regulatory submissions. *Drug Metabolism and Personalized Therapy*, 34 (2).

U.S. Department of Health and Human Services, FDA, 2017. In Vitro Metabolism- and Transporter-Mediated Drug-Drug Interaction Studies Guidance for Industry. *Interaction Studies*, 47.

U.S. Department of Health and Human Services, FDA, 2020. Guidance for Industry. *Interaction Studies*, 27.

Vainchenker, W., Leroy, E., Gilles, L., Marty, C., Plo, I., and Constantinescu, S.N., 2018. JAK inhibitors for the treatment of myeloproliferative neoplasms and other disorders. *F1000Research*, 7.

Wang, Z.-J., Yin, O.Q.P., Tomlinson, B., and Chow, M.S.S., 2008. OCT2 polymorphisms and in-vivo renal functional consequence: studies with metformin and cimetidine: *Pharmacogenetics and Genomics*, 18 (7), 637–645.

Zamek-Gliszczynski, M.J., Taub, M.E., Chothe, P.P., Chu, X., Giacomini, K.M., Kim, R.B., Ray, A.S., Stocker, S.L., Unadkat, J.D., Wittwer, M.B., Xia, C., Yee, S.-W., Zhang, L., Zhang, Y., and International Transporter Consortium, 2018. Transporters in Drug Development: 2018 ITC Recommendations for Transporters of Emerging Clinical Importance. *Clinical Pharmacology & Therapeutics*, 104 (5), 890–899.

Legends to figures

Figure 1. Interactions of ruxolitinib with OATs.

(A) Accumulation of reference substrates (6-CF for OAT1 and OAT3, E3S for OAT4) was determined in HEK-OAT cells incubated in the absence (control) or presence of ruxolitinib (10 or 100 μM) or of the reference OAT inhibitor probenecid (Prob) (2 mM). Data are expressed as % of substrate accumulation found in control cells, arbitrarily set at 100%, and are the means ± SD of three independent assays, each being performed in triplicate. **, $p < 0.01$ and ***, $p < 0.001$, when compared to control cells. (B) Effects of various concentrations of ruxolitinib on 6-CF-related OAT3 activity were analyzed in HEK-OAT3 cells with or without pre-incubation. Data are expressed as % of OAT3 activity in control cells not exposed to ruxolitinib, arbitrarily set at 100%; they are the means ± SD of three independent assays. IC_{50} values are indicated at the top of the graph. (C) Accumulation of ruxolitinib in HEK-OAT3 and HEK-MOCK cells exposed or not to 2 mM probenecid was determined by LC-MS/MS. Data are the means ± SD of three independent assays, each being performed in triplicate. NS, not statistically significant.

Figure 2. Effects of ruxolitinib on OATP activities.

(A) Accumulation of reference substrates (DCF for OATP1B1, 8-FcA for OATP1B3, DBF for OATP2B1) was determined in HEK-OATP cells incubated in the absence (control) or presence of ruxolitinib (10 or 100 μM) or of the reference OATP inhibitors BSP (100 μM) or rifamycin SV (Rif SV) (100 μM). Data are expressed as % of substrate accumulation found in control cells, arbitrarily set at 100%, and are the means ± SD of three independent assays, each being performed in triplicate. *, $p < 0.05$ and ***, $p < 0.001$, when compared to control cells. (B) Effects of various concentrations of ruxolitinib on DCF-related OATP1B1 activity were analyzed in HEK-OATP1B1 cells with or without pre-incubation with ruxolitinib. Data are

expressed as % of OATP1B1 activity in control cells not exposed to ruxolitinib, arbitrarily set at 100%; they are the means ± SD of three independent assays. IC_{50} values are indicated at the top of the graph.

Figure 3. Interactions of ruxolitinib with OCTs.

(A) Accumulation of the reference OCT substrate 4-Di-ASP was determined in HEK-OCT cells incubated in the absence (control) or presence of ruxolitinib (10 or 100 μM) or of the reference OCT inhibitors amitriptyline (Amitrip) (200 μM) or corticosterone (Cortico) (100 μM). Data are expressed as % of substrate accumulation found in control cells, arbitrarily set at 100%, and are the means ± SD of three independent assays, each being performed in triplicate. ***, $p < 0.001$, when compared to control cells. (B) Effects of various concentrations of ruxolitinib on OCT2 activity were analyzed in HEK-OCT2 cells with or without pre-incubation with ruxolitinib. Data are expressed as % of OCT2 activity in control cells not exposed to ruxolitinib, arbitrarily set at 100%; they are the means ± SD of three independent assays. IC_{50} values are indicated at the top of the graph. (C) Accumulation of ruxolitinib in HEK-OCT2 and HEK-MOCK cells exposed or not to 200 μM amitriptyline was determined by LC-MS/MS. Data are the means ± SD of three independent assays, each being performed in triplicate. NS, not statistically significant.

Figure 4. Interactions of ruxolitinib with MATEs.

(A) Accumulation of the reference MATE substrate TEA was determined in HEK-MATE cells incubated in the absence (control) or presence of ruxolitinib (10 or 100 μM) or of the reference MATE inhibitor verapamil (Vera) (200 μM). Data are expressed as % of substrate accumulation found in control cells, arbitrarily set at 100%, and are the means ± SD of three independent assays, each being performed in triplicate. ***, $p < 0.001$, when compared to control cells. (B)

Effects of various concentrations of ruxolitinib on MATE1 and MATE2-K activity were analyzed in HEK-MATE cells with or without pre-incubation with ruxolitinib. Data are expressed as % of MATE activity in control cells not exposed to ruxolitinib, arbitrarily set at 100%; they are the means ± SD of three independent assays. IC_{50} values are indicated at the top of the graphs. (C) Accumulation of ruxolitinib in HEK-MATE1, HEK-MATE2-K and HEK-MOCK cells exposed or not to 200 μM verapamil was determined by LC-MS/MS. Data are the means ± SD of three independent assays, each being performed in triplicate. *, $p < 0.05$, **, $p < 0.01$ and NS, not statistically significant.

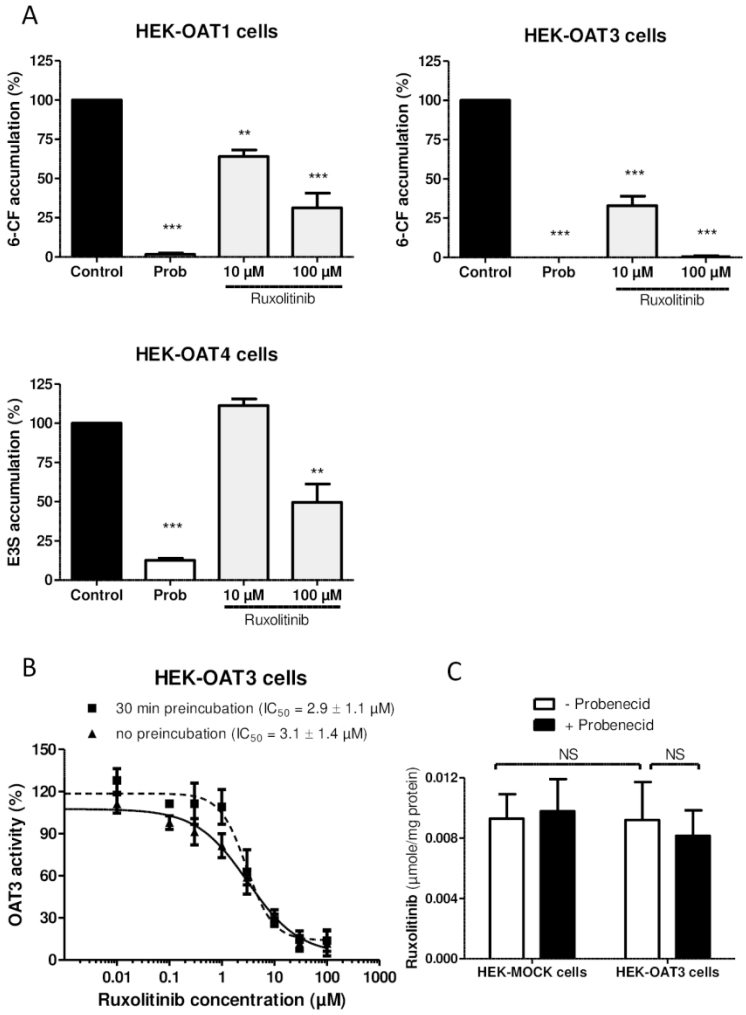

Figure 1. Interactions of ruxolitinib with OATs.
(A) Accumulation of reference substrates (6-CF for OAT1 and OAT3, E3S for OAT4) was determined in HEK-OAT cells incubated in the absence (control) or presence of ruxolitinib (10 or 100 µM) or of the reference OAT inhibitor probenecid (Prob) (2 mM). Data are expressed as % of substrate accumulation found in control cells, arbitrarily set at 100%, and are the means ± SD of three independent assays, each being performed in triplicate. **, $p < 0.01$ and ***, $p < 0.001$, when compared to control cells. (B) Effects of various concentrations of ruxolitinib on 6-CF-related OAT3 activity were analyzed in HEK-OAT3 cells with or without pre-incubation. Data are expressed as % of OAT3 activity in control cells not exposed to ruxolitinib, arbitrarily set at 100%; they are the means ± SD of three independent assays. IC50 values are indicated at the top of the graph (C) Accumulation of ruxolitinib in HEK-OAT3 and HEK-MOCK cells exposed or not to 2 mM probenecid was determined by LC-MS/MS. Data are the means ± SD of three independent assays, each being performed in triplicate. NS, not statistically significant.

209x289mm (200 x 200 DPI)

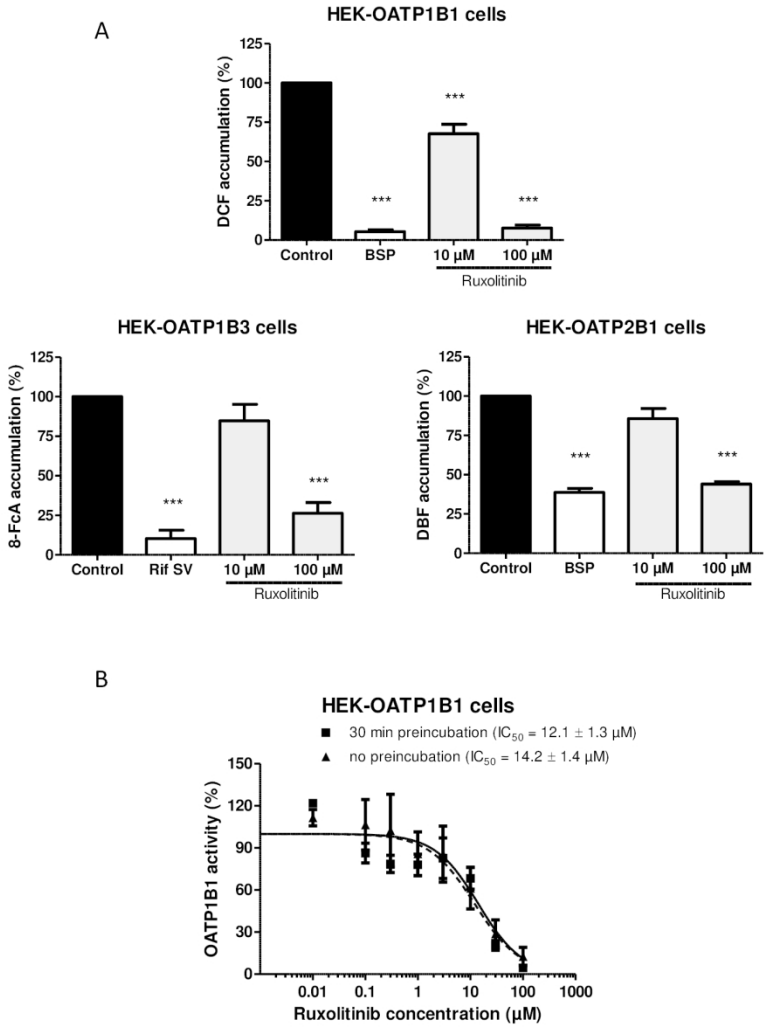

Figure 2. Effects of ruxolitinib on OATP activities.
(A) Accumulation of reference substrates (DCF for OATP1B1, 8-FcA for OATP1B3, DBF for OATP2B1) was determined in HEK-OATP cells incubated in the absence (control) or presence of ruxolitinib (10 or 100 µM) or of the reference OATP inhibitors BSP (100 µM) or rifamycin SV (Rif SV) (100 µM). Data are expressed as % of substrate accumulation found in control cells, arbitrarily set at 100%, and are the means ± SD of three independent assays, each being performed in triplicate. *, $p < 0.05$ and ***, $p < 0.001$, when compared to control cells. (B) Effects of various concentrations of ruxolitinib on DCF-related OATP1B1 activity were analyzed in HEK-OATP1B1 cells with or without pre-incubation with ruxolitinib. Data are expressed as % of OATP1B1 activity in control cells not exposed to ruxolitinib, arbitrarily set at 100%; they are the means ± SD of three independent assays. IC50 values are indicated at the top of the graph.

209x289mm (200 x 200 DPI)

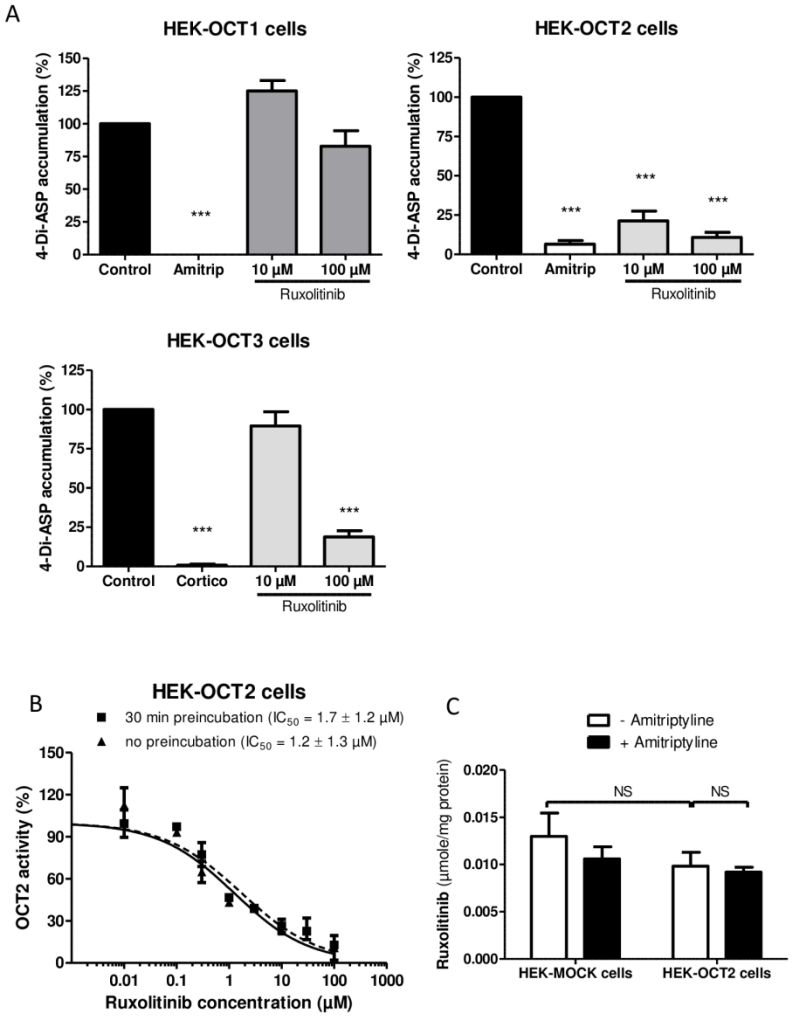

Figure 3. Interactions of ruxolitinib with OCTs.
(A) Accumulation of the reference OCT substrate 4-Di-ASP was determined in HEK-OCT cells incubated in the absence (control) or presence of ruxolitinib (10 or 100 µM) or of the reference OCT inhibitors amitriptyline (Amitrip) (200 µM) or corticosterone (Cortico) (100 µM). Data are expressed as % of substrate accumulation found in control cells, arbitrarily set at 100%, and are the means ± SD of three independent assays, each being performed in triplicate. ***, $p < 0.001$, when compared to control cells. (B) Effects of various concentrations of ruxolitinib on OCT2 activity were analyzed in HEK-OCT2 cells with or without pre-incubation with ruxolitinib. Data are expressed as % of OCT2 activity in control cells not exposed to ruxolitinib, arbitrarily set at 100%; they are the means ± SD of three independent assays. IC50 values are indicated at the top of the graph. (C) Accumulation of ruxolitinib in HEK-OCT2 and HEK-MOCK cells exposed or not to 200 µM amitriptyline was determined by LC-MS/MS. Data are the means ± SD of three independent assays, each being performed in triplicate. NS, not statistically significant.

209x289mm (200 x 200 DPI)

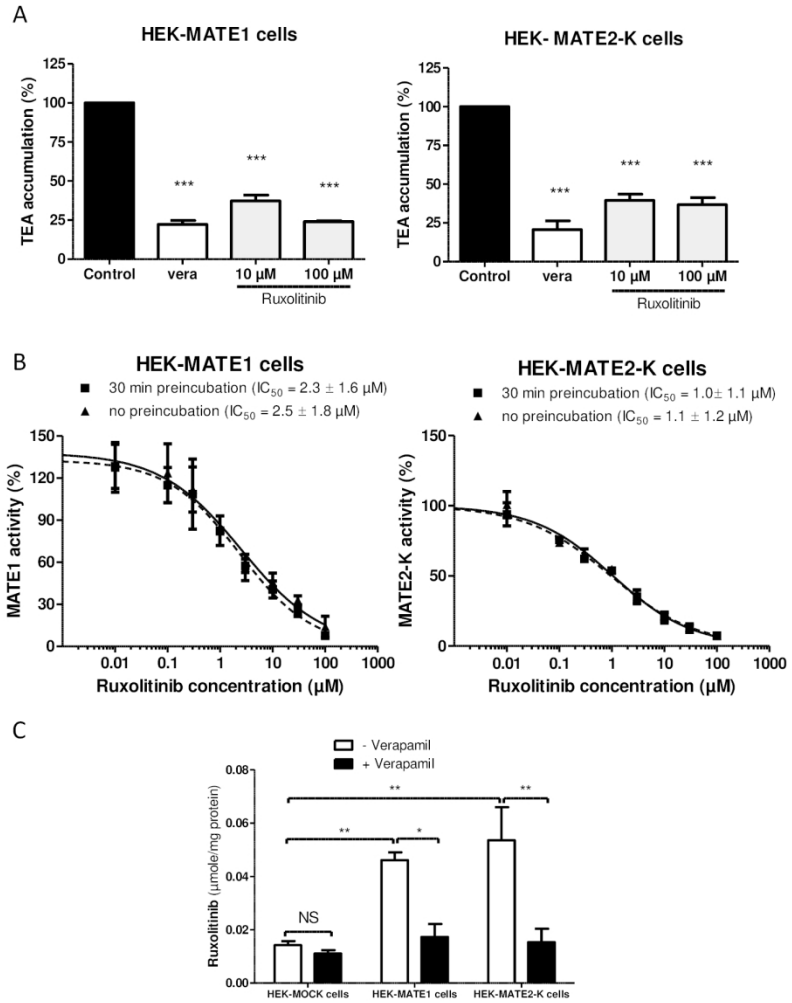

Figure 4. Interactions of ruxolitinib with MATEs.
(A) Accumulation of the reference MATE substrate TEA was determined in HEK-MATE cells incubated in the absence (control) or presence of ruxolitinib (10 or 100 µM) or of the reference MATE inhibitor verapamil (Vera) (200 µM). Data are expressed as % of substrate accumulation found in control cells, arbitrarily set at 100%, and are the means ± SD of three independent assays, each being performed in triplicate. ***, $p < 0.001$, when compared to control cells. (B) Effects of various concentrations of ruxolitinib on MATE1 and MATE2-K activity were analyzed in HEK-MATE cells with or without pre-incubation with ruxolitinib. Data are expressed as % of MATE activity in control cells not exposed to ruxolitinib, arbitrarily set at 100%; they are the means ± SD of three independent assays. IC50 values are indicated at the top of the graphs. (C) Accumulation of ruxolitinib in HEK-MATE1, HEK-MATE2-K and HEK-MOCK cells exposed or not to 200 µM verapamil was determined by LC-MS/MS. Data are the means ± SD of three independent assays, each being performed in triplicate. *, $p < 0.05$, **, $p < 0.01$ and NS, not statistically significant.

209x289mm (200 x 200 DPI)

Table 1: Summary of experimental conditions used for transporter activity assays

Transporter	Gene symbol	Cells	Substrate Method of analysis	Reference inhibitor
OATP1B1	*SLCO1B1*	HEK-OATP1B1	DCF (10.0 μM) Fluorimetry (492/517 nm)*	BSP (100 μM)
OATP1B3	*SLCO1B3*	HEK-OATP1B3	8-FcA (10.0 μM) Fluorimetry (485/535 nm)	BSP (100 μM)
OATP2B1	*SLCO2B1*	HEK-OATP2B1	DBF (10.0 μM) Fluorimetry (485/535 nm)	Rifamycin SV (100 μM)
OAT1	*SLC22A6*	HEK-OAT1	6-CF (10.0 μM) Fluorimetry (492/517 nm)	Probenecid (2 mM)
OAT3	*SLC22A8*	HEK-OAT3	6-CF (10.0 μM) Fluorimetry (492/517 nm)	Probenecid (2 mM)
OAT4	*SLC22A11*	HEK-OAT4	[^{3}H]-E3S (4.4 nM) Scintillation counting	Probenecid (2 mM)
OCT1	*SLC22A1*	HEK-OCT1	4-Di-ASP (10.0 μM) Fluorimetry (485/607 nm)	Amitriptyline (200 μM)
OCT2	*SLC22A2*	HEK-OCT2	4-Di-ASP (10.0 μM) Fluorimetry (485/607 nm)	Amitriptyline (200 μM)
MATE1	*SLC47A1*	HEK-MATE1	TEA (40.0 μM) LC-MS/MS	Verapamil (200 μM)
MATE2-K	*SLC47A2*	HEK-MATE2	TEA (40.0 μM) LC-MS/MS	Verapamil (200 μM)

Abbreviations: 6-CF, 6-carboxyfluorescein; 4-Di-ASP, 4-(4-(dimethylamino)styryl)-N-methylpyridinium iodide; BSP, sulfobromophthalein; DBF, 4′,5′-dibromofluorescein; DCF, 2′,7′-dichlorofluorescein; E3S, [6,7-3H(N)]-estrone-3-sulfate; LC-MS/MS, liquid chromatography-tandem mass spectroscopy; MATE, multidrug and toxin extrusion; OAT, organic anion transporter; OATP, organic anion transporter polypeptide; OCT, organic cation transporter; TEA, tetraethylammonium.

* Correspond to excitation/emission wavelengths.

Table 2: Prediction for *in vivo* inhibition of SLC transporter activity by ruxolitinib

Transporter	Ruxolitinib		IC_{50}[c]	$I_{max,u}/IC_{50}$	R value	Potential *in vivo* inhibition[d]
	$I_{max,u}$ (µM)[a]	$I_{in,max}$ (µM)[b]				
OAT1	0.216	17.7	> 10.0 µM	< 0.02	1.05	No inhibition
OAT3			3.1 µM	0.07		No inhibition
OAT4			> 10.0 µM	< 0.02		No inhibition
OATP1B1			> 10.0 µM			No inhibition
OATP1B3			> 10.0 µM			No inhibition
OATP2B1			> 10.0 µM			No inhibition
OCT1			> 100.0 µM			No inhibition
OCT2	0.216		1.4 µM	0.15		Risk of inhibition
OCT3			> 10.0 µM	< 0.02		No inhibition
MATE1			2.5 µM	0.09		No inhibition
MATE2K			1.1 µM	0.20		Risk of inhibition

[a]$I_{max,u}$ was calculated based on *in vivo* I_{max} (7.2 µM) and unbound fraction (0.03) described in US FDA data (Center for Drug Evaluation and Research 2011).

[b]$I_{in,max}$ was calculated with I_{max} value of 7.2 µM for a dosing of 200 mg according to Materials and Methods equation F and data from Umehara *et al.* 2019 (F_a = 0.99, F_g = 0.87, k_a = 2.02 h^{-1}, R_B = 1.2, Q_h= 90 L/h).

[c]IC_{50} values from the present study .

[d]defined and adapted according to the US FDA criteria for transporter-related DDI (based on equation D and E of Materials and Methods section). For US FDA-non regulatory transporters (OCT1, OAT4, OATP2B1 and OCT3), the equation D was applied for OAT4 and OCT3 and the equation E for OATP2B1 and OCT1.

Table 3. Comparison of data related to ruxolitinib-mediated *in vitro* inhibition of SLC transporters from the present study and from the FDA report for ruxolitinib (Center for Drug Evaluation and Research 2011).

Transporter	FDA report		Present study	
	Probe substrate[a]	Ruxolitinib effect	Probe substrate[a]	Ruxolitinib effect
OAT1	Aminohippuric acid	No inhibition (up to 37.5 μM)	6-CF	Inhibition (IC_{50}>10.0 μM)
OAT3	Estrone-3 sulfate	Inhibition (IC_{50}=6.5 μM)	6-CF	Inhibition (IC_{50}=3.1 μM)
OATP1B1	Estradiol-17βglucuronide	Inhibition (IC_{50}=19.3 μM)	DCF	Inhibition (IC_{50}>10.0 μM)
OATP1B3	Estradiol-17βglucuronide	Inhibition (IC_{50}=20.5 μM)	8-FcA	Inhibition (IC_{50}>10.0 μM)
OCT1	1-methyl-4-phenylpyridinium	Inhibition (IC_{50}=9.1 μM)	4-Di-ASP	No inhibition (up to 100.0 μM)
OCT2	1-methyl-4-phenylpyridinium	Inhibition (IC_{50}=9.8 μM)	4-Di-ASP	Inhibition (IC_{50}=1.2 μM)

[a]For each condition of IC_{50} determination, the used probe substrate is specified.

Supplemental data

Xenobiotica

Differential in vitro interactions of the Janus kinase inhibitor ruxolitinib with human SLC drug transporters

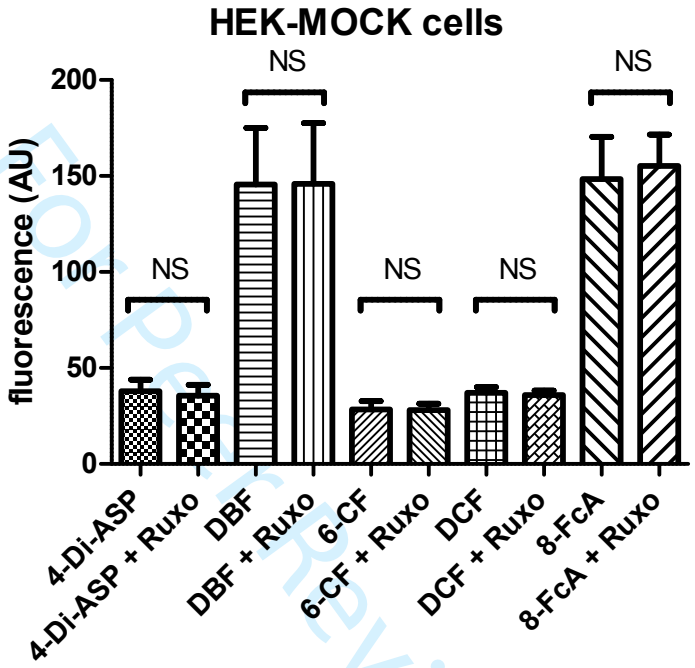

Figure S1: Lack of major analytical interaction of ruxolitinib (Ruxo) with fluorescent probes used as substrates for transporters. HEK-MOCK cells plated in 96 wells were either pre-treated or not with 100 µM ruxolitinib for 3 h; they were next incubated with the reference fluorescent probes 4 Di-ASP, DCF, DBF, 6-CF or 8-FcA (each at 10 µM) for 5 min. Probe-related fluorescence was then determined by spectrofluorimetry; data are expressed as arbitrary unit (AU)/wells and are the mean ± SEM of at least three assays. NS, not statistically significant.